

Axion-like particle limits from multi-messenger sources

Ariane Dekker,^{1,*} Gonzalo Herrera,^{2,†} and Dimitrios Kantzas^{3,‡}

¹*Kavli Institute for Cosmological Physics, The University of Chicago, Chicago, IL 60637 USA*

²*Center for Neutrino Physics, Department of Physics, Virginia Tech, Blacksburg, VA 24061, USA*

³*LAPTh, CNRS, USMB, F-74940 Annecy, France*

High-energy neutrino observation from the Seyfert galaxy NGC 1068 offers new insights into the non-thermal processes of active galactic nuclei. Simultaneous γ rays emitted by such sources can possibly oscillate into axion-like particles (ALPs) when propagating through astrophysical magnetic fields, potentially modifying the observed spectrum. To probe for ALP-induced signals, a robust understanding of the emission processes at the source is necessary. In this work, we perform a dedicated multi-messenger analysis by modeling a jet in the innermost vicinity of the central supermassive black hole of NGC 1068. We model in particular the neutrino and γ -ray emission originating in lepto-hadronic collisions between jet accelerated particles and background particles from the corona, reproducing both the Fermi-LAT and IceCube data. These source models serve as a baseline for ALP searches, and we derive limits on the ALP-photon coupling by marginalizing over motivated ranges of astrophysical parameters. We find $g_{a\gamma} \lesssim 7 \times 10^{-11} \text{GeV}^{-1}$ for $m_a \lesssim 10^{-9} \text{eV}$. These limits may be weaker than existing constraints, but they demonstrate the potential of multi-messenger observations to probe new physics. We conclude by discussing how additional upcoming multi-messenger sources and improved observational precision can enhance ALP sensitivity.

I. INTRODUCTION

Axion-Like Particles (ALPs) are light pseudoscalar bosons which arise in several extensions of the Standard Model, and can comprise the observed relic abundance of dark matter in the Universe [1–5]. Unlike the QCD axion, ALPs cannot resolve the strong CP problem, thereby spanning a wider parameter space and offering a richer phenomenology than the conventional axion. A generic feature of ALPs is their coupling to a two-photon vertex, which in the presence of an external magnetic field can lead to ALP-photon oscillations [6].

The ALP-photon coupling can modulate observations of γ -ray spectra from astrophysical sources with strong magnetic fields. Previous works have used this feature to set stringent limits on ALPs using observations from, for instance, Active Galactic Nuclei (AGN) [7–11], neutron stars [12, 13], supernovae [14–16], galaxy clusters [17–19] and using the magnetic field of the Milky Way’s galactic halo [20–24].

Probing ALPs using modulated γ -ray spectra from astrophysical sources requires a robust understanding of the intrinsic astrophysical emission processes. Multi-wavelength and multi-messenger observations help to reduce degeneracies between potential ALP signals and conventional astrophysical emission. For instance, astrophysical γ -ray attenuation typically leads to a lower energy flux enhancement, while ALP-induced attenuation is expected to suppress the flux across all wavelengths. Observing the spectral flux across all energy bands can therefore help identify the origin of the attenuation. Moreover, if the γ -ray emission is produced

from hadronic interactions, it is accompanied by a high-energy neutrino flux. Combining neutrino and γ -ray data therefore gives insights into dominant emission processes and might point towards additional mechanism such as ALP-induced effects.

IceCube has observed several high-energy (TeV-PeV) neutrinos in the past decade that might be associated with AGN. The first neutrino event that was found to be correlated with electromagnetic emission came from the flaring blazar TXS 0506+056 at 3.5σ significance [25, 26]. More recently, the IceCube collaboration reported an excess of 79_{-20}^{+22} neutrino events associated to nearby Seyfert type-2 galaxy NGC 1068 at 4.2σ level of significance [27], where Seyferts are the most abundant type of AGN. Interestingly, no emission has been observed in the TeV-range by MAGIC [28] while Fermi-LAT detected the source in the GeV-range [29, 30], and the overall γ -ray flux is at least an order of magnitude lower than expected. The lack of TeV γ -ray can be explained by γ rays being emitted in the innermost vicinity of the supermassive black hole (SMBH; $R_{\text{em}} \sim 10 - 100 R_S$, where R_S is the Schwarzschild radius: $2GM_{\text{BH}}/c^2$), which is an optical thick environment [31–37], together with an enhanced starburst activity farther away [38, 39]. Finally, it has been suggested that some beyond the Standard Model scenarios could also attenuate the γ -ray flux from NGC 1068, such as γ -ray oscillations into ALP, which subsequently decay into neutrinos [40], or dark matter scattering with photons and neutrinos [41, 42].

The observation of high-energy neutrinos from NGC 1068 led to dedicated searches of multi-messenger emission from other Seyfert galaxies [43, 44]. For instance, recent work by Ref. [45] found two 100 TeV neutrinos that coincide with the Seyfert galaxy NGC 7469 at 3.3σ level, while no significant excess was found by Fermi-LAT. Additional Seyfert type-2 sources are expected to be identified through ongoing IceCube obser-

* ahdekker@uchicago.edu

† gonzaloherrera@vt.de

‡ kantzas@lapth.cnrs.fr

vations, and upcoming data from IceCube-Gen2 [46], KM3NeT [47], P-ONE [48] and Baikal-GVD [49], combined with follow-up observations in γ rays, X-rays, UV and optical. This motivates us to explore the multi-messenger spectrum in the context of ALPs. Moreover, given the excess of 79 neutrino events associated with NGC 1068, this source offers a unique opportunity for detailed investigation.

In this work, we focus on NGC 1068 as a case study to describe its multi-messenger spectrum. We develop and discuss a jet model embedded in a thick corona to explain the γ -ray and neutrino emission. This model is consistent with observations and therefore enables us to search for dark matter induced modulations in the observed spectrum. We consider, in particular, γ -ray conversion into ALPs in the magnetic fields along the jets, finding $g_{a\gamma} \lesssim 7 \times 10^{-11} \text{GeV}^{-1}$ for $m_a \lesssim 10^{-9} \text{eV}$ at 95% CL. These limits are slightly weaker than existing limits, however, we discuss the potential improvement of these constraints if multiple NGC 1068-like sources are detected in γ rays. Such observations could improve upon current ALP bounds, demonstrating the power of multi-messenger analysis.

This work is structured as following. In Sec. II, we describe the jet model, and we calculate the neutrino and γ -ray emission by the innermost vicinity of the central SMBH of NGC 1068. In Sec. III, we investigate the γ -ray conversion into ALPs in the magnetic fields along the jets, and in Sec. IV we discuss the implications of our results.

II. JET MODEL

A. Expected astrophysical γ -ray and Neutrino Fluxes from NGC 1068

To calculate the γ -ray and neutrino emission from the accreting SMBH of NGC 1068, we adopt the jet model of [51], referred to as **BHJet**. This model accounts for the leptonic processes occurring along the jet, namely synchrotron emission of non-thermal electrons and inverse Compton scattering (ICS) with target photons, both originating in the jets and external photon fields. We further develop **BHJet** to account for hadronic processes of non-thermal protons according to Ref. [52] and we refer to this model as **HadJet**. We direct the interested reader to Refs.[51, 52] for detailed descriptions, however, we briefly describe the model below.

Two relativistic Poynting-flux dominated jets are launched by the accreting SMBH, perpendicular to the accretion plane, assuming that the two jets are identical. We assume that the jets are launched at a distance $2 R_g$ ($1 R_g \approx 1.5 \text{km} \times M_{\text{BH}}/M_\odot$) from the SMBH with a jet base of radius r_0 . Whereas the bulk kinetic energy is carried by thermal protons, the thermal electrons at the jet base populate a Maxwell-Jüttner (MJ) distribution in energies that peaks at 511 keV. The thermal electrons emit

synchrotron radiation that usually peak in the sub-keV regime.

While the jets propagate, they accelerate up to some maximum Lorentz factor while the magnetic energy converts to kinetic. At distance z_{diss} , the majority of the magnetic energy has dissipated to kinetic energy. At this distance, the jet magnetisation is determined by

$$\sigma_f = \frac{B^2}{4\pi n m_p c^2} < 1, \quad (1)$$

where B is the magnetic field strength and n is the particle number density. In this region, the majority of the power is carried by the particles. We assume that at z_{diss} , electrons and protons start to accelerate to non-thermal energies driven by particle acceleration mechanism [51]. We remain agnostic to the specific mechanism and we capture this phenomenon by assuming that non-thermal particles follow a power in energies with index p_e , which is the same for both electrons and protons. We further parametrise the efficiency of the particle acceleration mechanism assuming the relative timescale [53]

$$t_{\text{acc}}(E) = \frac{4E}{3f_{\text{sc}}ecB}, \quad (2)$$

where E is the particle energy, e is the particle charge, c is the speed of light and $f_{\text{sc}} < 1$. Equating the acceleration timescale to the energy loss timescales, we calculate the maximum attainable energy of non-thermal electrons and protons along the jets. Finally, we assume that particles accelerate to non-thermal energies along the jets from z_{diss} up to a maximum distance where the jets terminate in the intergalactic medium. This distance extends up to $10^8 R_g$, hence does not affect the γ -ray and neutrino emission. We capture jet physics assuming that the jets consist of 100 continuous segments from the jet base to the termination region.

The non-thermal particles radiate in the entire multi-wavelength spectrum. The leptonic particles emit synchrotron radiation that is further upscattered via ICS. Whereas these processes dominate the entire spectrum in many cases, for NGC 1068 they are subdominant and they only dominate in the sub-GeV spectrum. The accelerated protons, on the other hand, interact with cold protons of the jet and the corona, as well as the high-energy emission of the jet at the same jet segments, leading to proton-proton (pp) and photo-hadronic ($p\gamma$) processes, respectively. We calculate the resulting γ -ray and neutrino spectra following Ref. [54] for pp and Ref. [55] for $p\gamma$.

The SMBH with mass $M_{\text{BH}} = 8 \times 10^6 M_\odot$ [56, 57] of NGC 1068 is surrounded by a dense medium, known as the corona. Following Ref. [33], we set the number density of the cold corona particles at $n = 10^{11} \text{cm}^{-3}$, the optical depth at $\tau = 0.5$, and its extent radius at $z_{\text{diss}} = 50 R_g$. The corona of NGC 1068 acts as a target for the jet accelerated protons, namely the jet protons collide inelastically on the corona protons. To ensure that the particle acceleration inside the jet will occur in

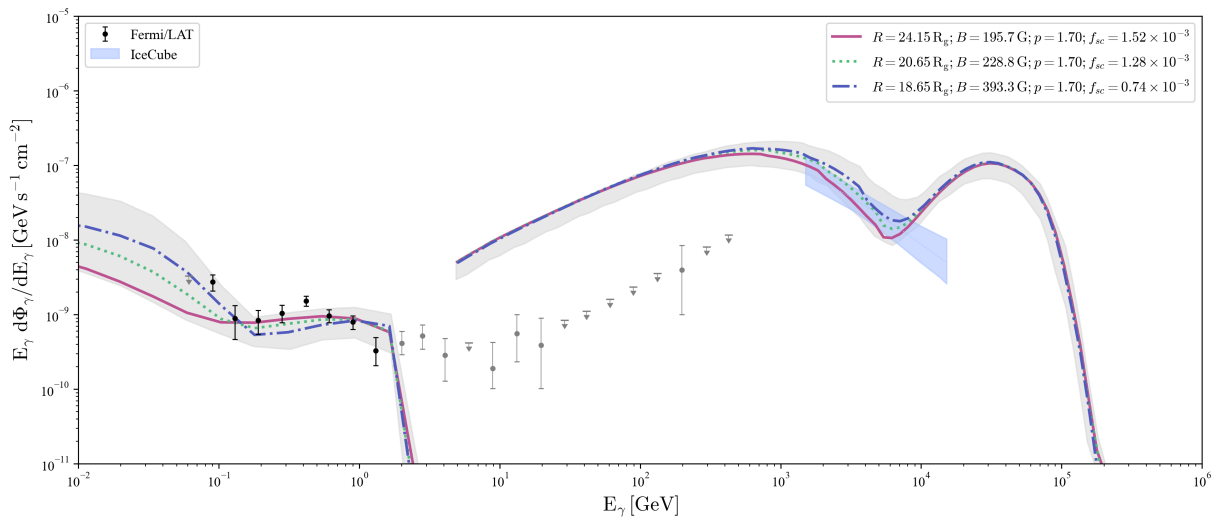


FIG. 1. SED of NGC 1068 focusing on the γ -ray regime and high-energy neutrinos, as measured by Fermi-LAT [29, 50] and IceCube [27]. The grey bands show the containment of the 10^6 HadJet simulations. We show 3 well-fitted individual models, where the pink line shows the best fit to the data. The resulting values of the free parameters R , p , f_{sc} and the calculated magnetic field strength from the magnetization σ_f are given in the legend.

a region which will be within the volume of the corona, we are only interested in values of $z_{\text{diss}} < R_{\text{cor}} = 50 R_g$. The dense corona acts also as a medium that attenuates the high-energy radiation produced at the jet, resulting in pair production, whereas the neutrinos produced by hadronic processes escape freely [32, 33, 36, 58].

B. Analysis

To constrain the jet dynamics of NGC 1068 and estimate the contribution of jet radiation in the high-energy regime, we fit HadJet to the Fermi-LAT data after selecting only models that reproduce IceCube measurements. In particular, we use the 15-year Fermi-LAT data from a $20^\circ \times 20^\circ$ region of interest surrounding NGC 1068 between 50 MeV and 500 GeV [50], as has been analyzed by Ref. [34].

In the Fermi-LAT analysis by Ref. [34], 14 energy bins are found that have both upper and lower limits on the energy spectrum. However, at the higher energy bins, an additional spectral contribution is expected from starburst activity farther away from the central engine, with supernova rates of $\sim 0.5 \text{ yr}^{-1}$ [38] (see also Ref. [59]), somewhat larger than expected from measurements of the Star Forming Rate [60]. It is beyond the scope of this work to model the starburst contribution, and we therefore only select the first 8 bins in the analysis that are expected to have a jet origin. Indeed, at larger energies, the emitted γ -ray flux is efficiently attenuated by ambient photons in the corona, inducing a strong cut-off.

We focus on two astrophysical free parameters that capture the jet morphology, namely the jet base radius r_0 , and the magnetization σ_f at the dissipation region

z_{diss} , which we set at $5 R_g$, well within the corona. To constrain the particle acceleration in the jets, we fit the power-law index of the non-thermal particles p_e and the particle acceleration efficiency f_{sc} . We then perform a χ^2 statistical analysis to fit the Fermi-LAT data, considering only models that are found to produce a neutrino flux that fall within the observed uncertainty band from the IceCube measurements [27]. More precisely, we minimize

$$\chi^2(r_0, \sigma_f, p_e, f_{sc}) = \sum_i \frac{(\Phi_{\gamma,i}(r_0, \sigma_f, p_e, f_{sc}) - \Phi_{\gamma,i}^{\text{obs}})^2}{(\delta\Phi_{\gamma,i}^{\text{obs}})^2}, \quad (3)$$

where the index i runs over the different bins in Fermi-LAT data from NGC 1068 in [29, 50]. We perform 10^6 simulations, varying the astrophysical parameters over the following motivated ranges: $r_0 = [5, 30] R_g$, $\sigma_f = [0.01, 1]$, $p_e = [1.6, 2.4]$, and $f_{sc} = [0.1, 20] \times 10^{-3}$.

C. Results

Figure 1 shows the Spectral Energy Distribution (SED) of the best-fit model (solid purple line), both for γ -ray and neutrino emission. We further show in dashed and dotted lines other well-fitted solutions, and the gray shaded bands contain all our 10^6 simulations of the expected γ -ray and high-energy neutrino emitted fluxes. First, we see that the Fermi-LAT spectrum can be well explained by pp γ rays, whereas ICS contributes in the sub-GeV regime. The emitted γ -ray spectrum is heavily attenuated by the corona, whereas the produced neutrinos propagate freely. In particular, the emitted neutrino spectrum has a double-bump shape due to the contribution of both pp (first peak) and p γ neutrinos (second

Parameter	Range of values	Best-fit value	Description
r_0/R_g	[5, 30]	24.15	Jet base radius
σ_f	[0.01, 1]	0.02	Magnetization at dissipation region (Eq. 1)
p_e	[1.6, 2.4]	1.7	Non-thermal power-law index $-\frac{\log(dn/dE)}{\log(dE)}$
f_{sc}	$[0.1, 20] \times 10^{-3}$	1.52×10^{-3}	Acceleration timescale factor
χ^2	≥ 23	23	Minimum χ^2 fitted to Fermi-LAT data
n/cm^{-3}	$[4, 222] \times 10^7$	10.13×10^7	Particle number density at dissipation region
B/G	[157, 4709]	196	Magnetic field strength at dissipation region

TABLE I. Description of the astrophysical free parameters we consider in **HadJet** and their ranges. Moreover, we show the best fit to NGC 1068 Fermi-LAT data and the obtained χ^2 values. The number density and the magnetic field are derived from the above parameters.

peak). We show the total neutrino and anti-neutrino spectrum per neutrino flavor and we compare it to the observed neutrino spectrum by IceCube (shaded blue region). The emitted neutrino signal falls well within the observed limit, with some minor excess in the ~ 10 TeV regime. Further observations could possibly prove this feature or constrain it. To calculate the event rate, we follow Ref. [61], accounting for the effective area of IceCube for zenith angles between -5 and $+30$ degrees. We find that 92 muon neutrino events are expected, in reasonable agreement with the IceCube reported number of 79 ± 20 events [27].

III. ALP-PHOTON OSCILLATION

The coupling of ALPs to photons is described by the Lagrangian,

$$\mathcal{L}_{a\gamma} = -\frac{1}{4}g_{a\gamma}F_{\mu\nu}\tilde{F}^{\mu\nu}a, \quad (4)$$

where $F_{\mu\nu}$ is the electromagnetic field tensor, $\tilde{F}^{\mu\nu}$ its dual, and a is the ALP field strength. The effective Lagrangian for the ALP-photon system is

$$\mathcal{L} = \mathcal{L}_{a\gamma} + \mathcal{L}_{\text{EH}} + \mathcal{L}_a, \quad (5)$$

where \mathcal{L}_{EH} is the Euler-Heisenberg Lagrangian accounting for one-loop corrections to the photon propagator, and the ALP Lagrangian terms are

$$\mathcal{L}_a = \frac{1}{2}\partial_\mu a \partial^\mu a - \frac{1}{2}m_a^2 a^2. \quad (6)$$

ALPs couple to photons in the presence of a magnetic field component transversal to the direction of propagation. The equations of motion for a photon beam with energy E read [6, 62]

$$\left(i\frac{d}{dz} + E + \mathcal{M}\right)\Psi(z) = 0, \quad (7)$$

with $\Psi(z) = (A_x(z), A_y(z), a(z))^T$, A 's being the polarization states along directions x and y and the mixing matrix \mathcal{M} reads

$$\mathcal{M} = \begin{pmatrix} \Delta_\perp & 0 & 0 \\ 0 & \Delta_\parallel & \Delta_{a\gamma} \\ 0 & \Delta_{a\gamma} & \Delta_a \end{pmatrix}. \quad (8)$$

QED vacuum polarization effects and the propagation of photons in the plasma medium give rise to the terms $\Delta_\perp = \Delta_{\text{pl}} + 2\Delta_{\text{QED}}$ and $\Delta_\parallel = \Delta_{\text{pl}} + 7/2\Delta_{\text{QED}}$, with $\Delta_{\text{pl}} = -\omega_{\text{pl}}/(2E)$ and the plasma frequency $\omega_{\text{pl}} \sim 0.037\sqrt{n}$, where n is the number density of electrons in the plasma. The QED vacuum polarization term reads $\Delta_{\text{QED}} = \alpha E/(45\pi)(B/(B_{\text{cr}}))^2$, with the fine-structure constant α , and the critical magnetic field $B_{\text{cr}} = m_e^2/|e| \sim 4.4 \times 10^{13}\text{G}$. The kinetic term for the ALP is $\Delta_a = -m_a^2/(2E)$ and photon-ALP mixing is given by the off-diagonal elements $\Delta_{a\gamma} = g_{a\gamma}B/2$. The above system of equations can be solved with the software **GammaALPs** for a combination of astrophysical environments, which allows obtaining the photon survival probability, hence, axion field opacity to γ rays as a function of energy [63]. As described in the previous section, we consider a jet-based mechanism for the acceleration of cosmic rays and production of high-energy neutrinos and γ rays. Thus, we consider the **GammaALPs** “Jet” model, where the ALP-photon mixing occurs in the toroidal magnetic field of the AGN jet. In this case, the magnetic field is modelled as a power-law in distance from the central black hole as

$$B(r) = B_0 \left(\frac{r}{R_{\text{em}}}\right)^{-1}, \quad (9)$$

where R_{em} is the emitting region of γ rays of the AGN. Similarly, the electron number density is modelled as a power-law function

$$n(r) = n_0 \left(\frac{r}{R_{\text{em}}}\right)^{-2}. \quad (10)$$

For the attenuation of γ rays in the Extragalactic Background Light, we use the model from Ref. [64]. Fi-

nally, we also consider the possibility of ALP-photon conversions in the coherent component of the magnetic field of the Milky Way. In that case, the magnetic field model is taken from Refs. [65, 66], and the number density of electrons is constant [67].

Under this prescription, we can compute the attenuated γ -ray flux due to ALP-photon oscillations as

$$\frac{d\Phi_{\gamma}^{\text{att}}}{dE_{\gamma}} = \frac{d\Phi_{\gamma}}{dE_{\gamma}} P_{a\gamma}(E_{\gamma}, m_a, g_{a\gamma}, \theta_{\text{astro}}), \quad (11)$$

where $\Phi_{\gamma}^{\text{att}}$ is the attenuated γ -ray flux and Φ_{γ} the expected γ -ray flux from the accreting SMBH of NGC 1068. $P_{a\gamma}$ is the ALP-photon oscillation that depends on the γ -ray energy E_{γ} , axion mass m_a , axion-photon coupling $g_{a\gamma}$, and the range of astrophysical parameters θ_{astro} as discussed in the next section.

A. ALP analysis

We derive limits on the ALP parameter space, and identify ALP regions that better fit the Fermi-LAT and IceCube data. We perform a profile likelihood analysis by marginalizing over the astrophysical nuisance parameters $\theta_{\text{astro}} = (r_0, \sigma_f, p_e, f_{\text{sc}})$ that predict different SED, as illustrated in Fig. 1 as a gray band. For each value $(m_a, g_{a\gamma})$, we compute $\chi^2(m_a, g_{a\gamma}; \theta_{\text{astro}})$ by minimizing over the nuisance parameters, where $\chi^2(m_a, g_{a\gamma}; \theta_{\text{astro}})$ is obtained through a least-squares analysis using the Fermi-LAT data of NGC 1068. We obtain 95% CL limits on $g_{a\gamma}$ as a function of m_a through a Likelihood-Ratio analysis, which follows Ref. [68]

$$\chi^2(m_a, g_{a\gamma}; \theta_{\text{astro}}) - \chi_{\text{min}}^2(\theta_{\text{astro}}) = \Delta\chi^2 \leq 2.71. \quad (12)$$

The considered ranges for the nuisance parameters are shown in Table I.

B. Results

Figure 2 shows the best-fit expected γ -ray and neutrino emission in solid purple lines, together with the unattenuated emission (dotted purple line) for illustration purposes. We further show in a dashed orange line the additionally attenuated γ -ray flux induced by ALP-photon oscillation effects in the magnetic field of the jets of NGC 1068, for benchmark values of the ALP mass $m_a = 10^{-7}$ eV and axion-photon coupling $g_{a\gamma} = 10^{-10}$ GeV $^{-2}$. We see that the ALP-photon oscillation can sizably deplete the γ -ray flux below observational levels. This feature can be used to set limits on the ALP-photon coupling and mass.

We find a best-fit point in the ALP parameter space at $(m_a, g_{a\gamma}) = (2.2 \times 10^{-9} \text{ GeV}^{-1}, 4.6 \times 10^{-10} \text{ eV})$, corresponding to a significance of only 1.02σ , indicating no meaningful preference.

In Fig. 3, we show the ALP-photon coupling versus the ALP mass. The solid blue line corresponds to the

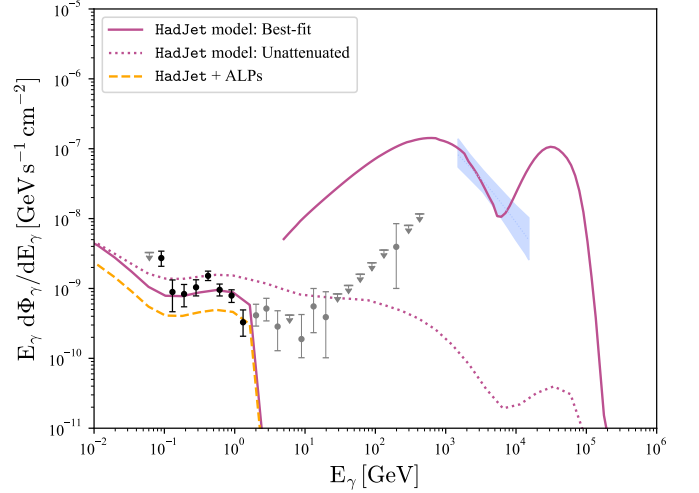


FIG. 2. SED of NGC 1068, including γ -ray measurements from Fermi-LAT [29, 50], high-energy neutrino measurements from IceCube [27], and the best-fit model (solid purple line). The opaque γ -ray flux due to ALP-photon oscillations in the jet of NGC 1068 is shown as orange dashed line with ALP parameters $m_a = 10^{-7}$ eV and $g_{a\gamma} = 10^{-10}$ GeV $^{-1}$.

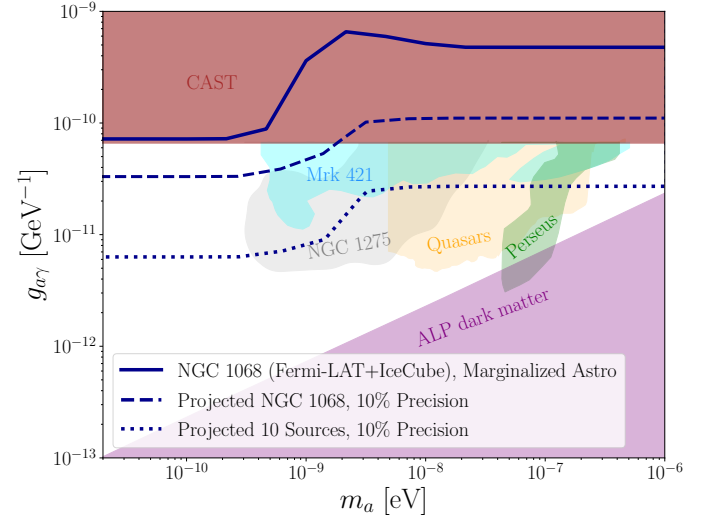


FIG. 3. Upper limits on the ALP-photon coupling versus ALP mass by marginalizing over astrophysical parameters described in Table I (solid blue line). We further show projected limits with improved Fermi-LAT precision of 10% (dashed blue line), and from the observation of 10 NGC 1068-like sources with 10% precision (dotted blue line). We compare with previous results [19, 69–71], and show the region where ALPs have the correct relic abundance via the misalignment mechanism (shaded purple) [72].

95% CL limits obtained when marginalizing over the astrophysical parameters. Moreover, we compare our lim-

its to previous bounds arising from ALP-photon oscillations in γ -ray astrophysical sources. In particular, we show bounds from the combination of ARGO-YBJ and Fermi-LAT observations of the blazar Mrk 421 (dashed cyan region) [69], Fermi-LAT observations of NGC 1275 (dashed gray region) [70], flat-spectrum radio quasars observed with Fermi-LAT (dashed orange region) [71], and observations of the Perseus Galaxy with MAGIC (dashed green region) [28]. We also show the bound obtained by the CAST experiment at CERN, based on solar ALP-photon conversions in the presence of a strong magnetic field in the laboratory [73].

It should be noted that additional limits exist on the ALP-photon coupling from ALP production and reconversion into X-rays from ALP-induced polarization effects, and from reionization probes, *e.g.* [23, 40, 69, 74–80]. We further show the region of parameter space where ALPs can constitute the dark matter of the Universe (shaded purple region) [72].

Figure 3 also illustrates projected limits from NGC 1068 with improved precision of 10% in the measurements (dashed blue line), and projected limits with the observation of 10 NGC 1068-like sources and 10% precision in each of the measurements (dotted blue line). This would constitute an improvement w.r.t to current measurements from Fermi-LAT, which present uncertainties in the range 16.7% – 50%, depending on the energy bin considered. We generate mock astrophysical predictions and data by performing a 1σ Gaussian perturbation of the best-fit astrophysical flux from NGC 1068 discussed in Sec. II, together with the central values of the measurements of Fermi-LAT data. We note that using the best-fit astrophysical model instead of marginalizing over astrophysical parameters improves the limits by $< 20\%$. The mock astrophysical fluxes and corresponding observed data are then generated as

$$\Phi_{\gamma,i}^{\text{mock(obs)}}(E_i) = \Phi_{\gamma,i}^{\text{(obs)}}(E_i) \times (1 + \delta_i), \quad \delta_i \sim \mathcal{N}(0, 1), \quad (13)$$

where $\mathcal{N}(0, 1)$ denotes a Gaussian distribution centered at $\mu = 0$ with standard deviation $\sigma = 0.1$. Under this prescription, and fixing the uncertainty in mock data to 10% in every energy bin, we find that our limits could significantly improve previous limits from γ -ray sources for some values of the ALP mass. We note that measurement uncertainties of 10% have been obtained for other Fermi-LAT sources in the 20–500 GeV energy-range, and future experiments like AMEGO [81], e-Astrogram [82] or CTAO [83] are expected to improve over Fermi-LAT precision.

IV. DISCUSSION

The multi-messenger era brings us the opportunity to understand the underlying processes leading to the observed γ -ray and high-energy neutrino fluxes from distant astrophysical sources. In this context, beyond the

Standard Model scenarios may induce modifications of the emitted astrophysical γ -ray or neutrino fluxes, leaving the former or the latter unaltered. ALP-photon oscillations is a widely discussed possibility to modify the γ -ray flux from extragalactic sources, like AGNs. We propose to use multi-messenger sources that are observed in high-energy neutrinos, as they offer a unique opportunity to disentangle intrinsic emission mechanism from ALP-induced effects. This enables to derive robust limits on the ALP-photon coupling.

For this purpose, we develop a model that allows for lepto-hadronic processes between jet accelerated protons and cold target particles of the corona. Using this model, we calculate the expected γ -ray and high-energy neutrino fluxes from NGC 1068, and compare to IceCube and Fermi-LAT data. The observation of high-energy neutrinos by IceCube significantly constrains the astrophysical parameter space allowing for more robust conclusions on the origin of the non-thermal emission. We find that ICS of jet accelerated electrons can reproduce the sub-GeV spectrum, pp inelastic collisions between accelerated jet protons and corona thermal protons can contribute or even dominate the GeV spectrum, whereas neutrinos from both pp and $p\gamma$ interactions can explain the ~ 80 events detected by IceCube. The entire high-energy γ -ray emission is suppressed due to the optical thick corona.

Using these simulations, we derive limits on the ALP-photon coupling, at the level of $g_{a\gamma} \lesssim 7 \times 10^{-11} \text{GeV}^{-1}$ for $m_a \lesssim 10^{-9} \text{eV}$. These limits are weaker than previous analyses of astrophysical γ -ray sources. However, we expect that with a population of 10 NGC 1068-like sources and considering an improved precision in future γ -ray measurements of 10%, to find comparable and complementary limits when compared to current results from γ -ray sources.

Our analysis can be extended in several ways. One may consider different γ -ray sources, such as TXS or PKS blazars, which have also been observed in γ rays and high-energy neutrinos [25]. Furthermore, other Seyfert galaxies have been observed by IceCube with moderate significance [44], and while Fermi-LAT currently does not find a significant γ -ray flux, future observations could improve the limits. Beyond the Standard Model scenarios could be considered as attenuating media in these sources. We expect future multi-messenger and multi-wavelength observations to help determine the dark opacity of the Universe to γ rays.

V. ACKNOWLEDGMENTS

We thank Francesca Calore and Marco Chianese for valuable comments on the draft. AD is supported by the Kavli Institute for Cosmological physics at the University of Chicago through an endowment from the Kavli Foundation and its founder Fred Kavli. The work of GH is supported by the U.S. Department of Energy un-

der award number DE-SC0020262. DK acknowledges funding from the French Programme d'investissements

d'avenir through the Enigmass Labex, and from the 'Agence Nationale de la Recherche', grant number ANR-19-CE310005-01 (PI: F. Calore).

-
- [1] R. D. Peccei and H. R. Quinn, CP Conservation in the Presence of Instantons, *Phys. Rev. Lett.* **38**, 1440 (1977).
 - [2] S. Weinberg, A New Light Boson?, *Phys. Rev. Lett.* **40**, 223 (1978).
 - [3] J. Preskill, M. B. Wise, and F. Wilczek, Cosmology of the Invisible Axion, *Phys. Lett. B* **120**, 127 (1983).
 - [4] D. J. Marsh, Axion cosmology, *Physics Reports* **643**, 1–79 (2016).
 - [5] A. Arvanitaki, S. Dimopoulos, S. Dubovsky, N. Kaloper, and J. March-Russell, String axiverse, *Physical Review D* **81**, 10.1103/physrevd.81.123530 (2010).
 - [6] G. Raffelt and L. Stodolsky, Mixing of the photon with low-mass particles, *Phys. Rev. D* **37**, 1237 (1988).
 - [7] D. Hooper and P. D. Serpico, Detecting Axion-Like Particles With Gamma Ray Telescopes, *Phys. Rev. Lett.* **99**, 231102 (2007), arXiv:0706.3203 [hep-ph].
 - [8] C. S. Reynolds, M. C. David Marsh, H. R. Russell, A. C. Fabian, R. Smith, F. Tombesi, and S. Veilleux, Astrophysical limits on very light axion-like particles from chandra grating spectroscopy of ngc 1275, *The Astrophysical Journal* **890**, 59 (2020).
 - [9] J. Sisk-Reynés, J. H. Matthews, C. S. Reynolds, H. R. Russell, R. N. Smith, and M. C. D. Marsh, New constraints on light axion-like particles using chandra transmission grating spectroscopy of the powerful cluster-hosted quasar h1821+643, *Monthly Notices of the Royal Astronomical Society* **510**, 1264–1277 (2021).
 - [10] S. Jacobsen, T. Linden, and K. Freese, Constraining axion-like particles with hawc observations of tev blazars (2022), arXiv:2203.04332 [hep-ph].
 - [11] A. Abramowski *et al.* (H.E.S.S.), Constraints on axion-like particles with H.E.S.S. from the irregularity of the PKS 2155-304 energy spectrum, *Phys. Rev. D* **88**, 102003 (2013), arXiv:1311.3148 [astro-ph.HE].
 - [12] F. Lecce, A. Lella, G. Lucente, V. Vijayan, A. Bauswein, M. Giannotti, and A. Mirizzi, Probing axion-like particles with multimessenger observations of neutron star mergers (2025), arXiv:2504.02032 [hep-ph].
 - [13] M. Diamond, D. F. G. Fiorillo, G. Marques-Tavares, I. Tamborra, and E. Vitagliano, Multimessenger Constraints on Radiatively Decaying Axions from GW170817, *Phys. Rev. Lett.* **132**, 101004 (2024), arXiv:2305.10327 [hep-ph].
 - [14] F. Calore, P. Carenza, C. Eckner, T. Fischer, M. Giannotti, J. Jaeckel, K. Kotake, T. Kuroda, A. Mirizzi, and F. Sivo, 3d template-based fermi-lat constraints on the diffuse supernova axion-like particle background, *Physical Review D* **105**, 10.1103/physrevd.105.063028 (2022).
 - [15] F. R. Candón, S. Ganguly, M. Giannotti, T. Kumar, A. Lella, and F. Mescia, A fresh look at the diffuse alp background from supernova (2025), arXiv:2505.05567 [hep-ph].
 - [16] M. Meyer, M. Giannotti, A. Mirizzi, J. Conrad, and M. A. Sánchez-Conde, Fermi Large Area Telescope as a Galactic Supernovae Axionscope, *Phys. Rev. Lett.* **118**, 011103 (2017), arXiv:1609.02350 [astro-ph.HE].
 - [17] M. H. Chan, Constraining the axion-photon coupling using radio data of the bullet cluster (2021), arXiv:2109.11734 [astro-ph.CO].
 - [18] M. Schleder and G. Sigl, Constraining alp-photon coupling using galaxy clusters, *Journal of Cosmology and Astroparticle Physics* **2016** (01), 038–038.
 - [19] H. Abe *et al.* (MAGIC), Constraints on axion-like particles with the Perseus Galaxy Cluster with MAGIC, *Phys. Dark Univ.* **44**, 101425 (2024), arXiv:2401.07798 [astro-ph.HE].
 - [20] M. Simet, D. Hooper, and P. D. Serpico, The Milky Way as a Kiloparsec-Scale Axionscope, *Phys. Rev. D* **77**, 063001 (2008), arXiv:0712.2825 [astro-ph].
 - [21] J. P. Conlon and F. V. Day, 3.55 kev photon lines from axion to photon conversion in the milky way and m31, *Journal of Cosmology and Astroparticle Physics* **2014** (11), 033–033.
 - [22] P. Carenza, C. Evoli, M. Giannotti, A. Mirizzi, and D. Montanino, Turbulent axion-photon conversions in the milky way, *Physical Review D* **104**, 10.1103/physrevd.104.023003 (2021).
 - [23] C. Eckner and F. Calore, First constraints on axionlike particles from Galactic sub-PeV gamma rays, *Phys. Rev. D* **106**, 083020 (2022), arXiv:2204.12487 [astro-ph.HE].
 - [24] L. Mastrototaro, P. Carenza, M. Chianese, D. F. G. Fiorillo, G. Miele, A. Mirizzi, and D. Montanino, Constraining axion-like particles with the diffuse gamma-ray flux measured by the Large High Altitude Air Shower Observatory, *Eur. Phys. J. C* **82**, 1012 (2022), arXiv:2206.08945 [hep-ph].
 - [25] M. G. Aartsen *et al.* (IceCube, Fermi-LAT, MAGIC, AGILE, ASAS-SN, HAWC, H.E.S.S., INTEGRAL, Kanata, Kiso, Kapteyn, Liverpool Telescope, Subaru, Swift NuSTAR, VERITAS, VLA/17B-403), Multimessenger observations of a flaring blazar coincident with high-energy neutrino IceCube-170922A, *Science* **361**, eaat1378 (2018), arXiv:1807.08816 [astro-ph.HE].
 - [26] M. G. Aartsen *et al.* (IceCube), Neutrino emission from the direction of the blazar TXS 0506+056 prior to the IceCube-170922A alert, *Science* **361**, 147 (2018), arXiv:1807.08794 [astro-ph.HE].
 - [27] R. Abbasi *et al.* (IceCube), Evidence for neutrino emission from the nearby active galaxy NGC 1068, *Science* **378**, 538 (2022), arXiv:2211.09972 [astro-ph.HE].
 - [28] V. A. Acciari *et al.* (MAGIC), Constraints on gamma-ray and neutrino emission from NGC 1068 with the MAGIC telescopes, *Astrophys. J.* **883**, 135 (2019), arXiv:1906.10954 [astro-ph.HE].
 - [29] S. Abdollahi *et al.* (Fermi-LAT), *Fermi* Large Area Telescope Fourth Source Catalog, *Astrophys. J. Suppl.* **247**, 33 (2020), arXiv:1902.10045 [astro-ph.HE].
 - [30] M. Ajello *et al.* (Fermi-LAT), The Fourth Catalog of Active Galactic Nuclei Detected by the Fermi Large Area Telescope, *Astrophys. J.* **892**, 105 (2020), arXiv:1905.10771 [astro-ph.HE].

- [31] K. Murase, S. S. Kimura, and P. Meszaros, Hidden Cores of Active Galactic Nuclei as the Origin of Medium-Energy Neutrinos: Critical Tests with the MeV Gamma-Ray Connection, *Phys. Rev. Lett.* **125**, 011101 (2020), arXiv:1904.04226 [astro-ph.HE].
- [32] Y. Inoue, D. Khangulyan, and A. Doi, On the origin of high-energy neutrinos from ngc 1068: The role of non-thermal coronal activity, *The Astrophysical Journal* **891**, L33 (2020).
- [33] K. Murase, Hidden Hearts of Neutrino Active Galaxies, *Astrophys. J. Lett.* **941**, L17 (2022), arXiv:2211.04460 [astro-ph.HE].
- [34] C. Blanco, D. Hooper, T. Linden, and E. Pinetti, On the neutrino and gamma-ray emission from ngc 1068 (2023), arXiv:2307.03259 [astro-ph.HE].
- [35] D. F. G. Fiorillo, M. Petropoulou, L. Comisso, E. Peretti, and L. Sironi, TeV Neutrinos and Hard X-Rays from Relativistic Reconnection in the Corona of NGC 1068, *Astrophys. J.* **961**, L14 (2024), arXiv:2310.18254 [astro-ph.HE].
- [36] D. F. G. Fiorillo, L. Comisso, E. Peretti, M. Petropoulou, and L. Sironi, A magnetized strongly turbulent corona as the source of neutrinos from ngc 1068, *The Astrophysical Journal* **974**, 75 (2024).
- [37] P. Padovani *et al.*, High-energy neutrinos from the vicinity of the supermassive black hole in NGC 1068, *Nature Astron.* **8**, 1077 (2024), arXiv:2405.20146 [astro-ph.HE].
- [38] B. Eichmann, F. Oikonomou, S. Salvatore, R.-J. Dettmar, and J. Becker Tjus, Solving the Multimessenger Puzzle of the AGN-starburst Composite Galaxy NGC 1068, *Astrophys. J.* **939**, 43 (2022), arXiv:2207.00102 [astro-ph.HE].
- [39] A. B. Romeo and K. Fathi, What powers the starburst activity of NGC 1068? Star-driven gravitational instabilities caught in the act, *Mon. Not. Roy. Astron. Soc.* **460**, 2360 (2016), arXiv:1602.03049 [astro-ph.GA].
- [40] B. P. Pant, Constraining axionlike particles with invisible neutrino decay using the IceCube observations of NGC 1068, *Phys. Rev. D* **109**, 063002 (2024), arXiv:2311.14597 [astro-ph.HE].
- [41] G. Herrera, Plausible indication of gamma-ray absorption by dark matter in ngc 1068 (2025), arXiv:2504.21560 [hep-ph].
- [42] J. M. Cline and M. Puel, NGC 1068 constraints on neutrino-dark matter scattering, *JCAP* **06**, 004, arXiv:2301.08756 [hep-ph].
- [43] A. Neronov, D. Savchenko, and D. Semikoz, Neutrino signal from a population of seyfert galaxies, *Physical Review Letters* **132**, 10.1103/physrevlett.132.101002 (2024).
- [44] R. Abbasi *et al.* (IceCube), Search for Neutrino Emission from Hard X-Ray AGN with IceCube, *Astrophys. J.* **981**, 131 (2025), arXiv:2406.06684 [astro-ph.HE].
- [45] G. Sommani, A. Franckowiak, M. Lincetto, and R.-J. Dettmar, Two 100 TeV Neutrinos Coincident with the Seyfert Galaxy NGC 7469, *Astrophys. J.* **981**, 103 (2025), arXiv:2403.03752 [astro-ph.HE].
- [46] M. G. Aartsen *et al.* (IceCube-Gen2), IceCube-Gen2: the window to the extreme Universe, *J. Phys. G* **48**, 060501 (2021), arXiv:2008.04323 [astro-ph.HE].
- [47] S. Adrian-Martinez *et al.* (KM3Net), Letter of intent for KM3NeT 2.0, *J. Phys. G* **43**, 084001 (2016), arXiv:1601.07459 [astro-ph.IM].
- [48] M. Agostini *et al.* (P-ONE), The Pacific Ocean Neutrino Experiment, *Nature Astron.* **4**, 913 (2020), arXiv:2005.09493 [astro-ph.HE].
- [49] A. D. Avrorin *et al.* (Baikal-GVD), Neutrino Telescope in Lake Baikal: Present and Future, *PoS ICRC2019*, 1011 (2020), arXiv:1908.05427 [astro-ph.HE].
- [50] M. Ackermann *et al.* (Fermi-LAT), GeV Observations of Star-forming Galaxies with the Fermi Large Area Telescope, *Astrophys. J.* **755**, 164 (2012), arXiv:1206.1346 [astro-ph.HE].
- [51] M. Lucchini, C. Ceccobello, S. Markoff, Y. Kini, A. Chhotray, R. M. T. Connors, P. Crumley, H. Falcke, D. Kantzas, and D. Maitra, Bhjet: a public multizone, steady state jet + thermal corona spectral model, *MNRAS* **517**, 5853 (2022).
- [52] D. Kantzas, S. Markoff, T. Beuchert, M. Lucchini, A. Chhotray, C. Ceccobello, A. J. Tetarenko, J. C. A. Miller-Jones, M. Bremer, J. A. Garcia, V. Grinberg, P. Uttley, and J. Wilms, A new lepto-hadronic model applied to the first simultaneous multiwavelength data set for Cygnus X-1, *MNRAS* **500**, 2112 (2021).
- [53] J. Jokipii, Rate of energy gain and maximum energy in diffusive shock acceleration, *ApJ* **313**, 842 (1987).
- [54] S. Kelner, F. A. Aharonian, and V. Bugayov, Energy spectra of gamma rays, electrons, and neutrinos produced at proton-proton interactions in the very high energy regime, *Physical Review D* **74**, 034018 (2006).
- [55] S. Kelner and F. Aharonian, Energy spectra of gamma rays, electrons, and neutrinos produced at interactions of relativistic protons with low energy radiation, *Physical Review D* **78**, 034013 (2008).
- [56] J.-H. Woo and C. M. Urry, AGN black hole masses and bolometric luminosities, *Astrophys. J.* **579**, 530 (2002), arXiv:astro-ph/0207249.
- [57] F. Panessa, L. Bassani, M. Cappi, M. Dadina, X. Barcons, F. J. Carrera, L. C. Ho, and K. Iwasawa, On the X-ray, optical emission line and black hole mass properties of local Seyfert galaxies, *Astron. Astrophys.* **455**, 173 (2006), arXiv:astro-ph/0605236.
- [58] D. Karavola, M. Petropoulou, D. F. G. Fiorillo, L. Comisso, and L. Sironi, Neutrino and pair creation in reconnection-powered coronae of accreting black holes (2025), arXiv:2410.12638 [astro-ph.HE].
- [59] M. Ajello, K. Murase, and A. McDaniel, Disentangling the Hadronic Components in NGC 1068, *Astrophys. J. Lett.* **954**, L49 (2023), arXiv:2307.02333 [astro-ph.HE].
- [60] J. J. Condon, Radio emission from normal galaxies, *Ann. Rev. Astron. Astrophys.* **30**, 575 (1992).
- [61] D. Kantzas, S. Markoff, A. J. Cooper, D. Gaggero, M. Petropoulou, and P. De La Torre Luque, Possible contribution of X-ray binary jets to the Galactic cosmic ray and neutrino flux, *MNRAS* **524**, 1326 (2023).
- [62] A. De Angelis, G. Galanti, and M. Roncadelli, Relevance of axion-like particles for very-high-energy astrophysics, *Phys. Rev. D* **84**, 105030 (2011), [Erratum: *Phys. Rev. D* **87**, 109903 (2013)], arXiv:1106.1132 [astro-ph.HE].
- [63] M. Meyer, J. Davies, and J. Kuhlmann, gammaALPs: An open-source python package for computing photon-axion-like-particle oscillations in astrophysical environments, *PoS ICRC2021*, 557 (2021), arXiv:2108.02061 [astro-ph.HE].
- [64] A. Domínguez, J. R. Primack, D. J. Rosario, F. Prada, R. C. Gilmore, S. M. Faber, D. C. Koo, R. S. Somerville, M. A. Pérez-Torres, P. Pérez-González, J.-S. Huang, M. Davis, P. Guhathakurta, P. Barmby, C. J. Conselice, M. Lozano, J. A. Newman, and M. C. Cooper, Extra-

- galactic background light inferred from aegis galaxy-sed-type fractions: Ebl from aegis galaxy-sed-type fractions, *Monthly Notices of the Royal Astronomical Society* **410**, 2556–2578 (2010).
- [65] M. S. Pshirkov, P. G. Tinyakov, P. P. Kronberg, and K. J. Newton-McGee, Deriving the global structure of the galactic magnetic field from faraday rotation measures of extragalactic sources, *The Astrophysical Journal* **738**, 192 (2011).
- [66] R. Jansson and G. R. Farrar, A new model of the galactic magnetic field, *The Astrophysical Journal* **757**, 14 (2012).
- [67] D. Horns, L. Maccione, M. Meyer, A. Mirizzi, D. Montanino, and M. Roncadelli, Hardening of TeV gamma spectrum of AGNs in galaxy clusters by conversions of photons into axion-like particles, *Phys. Rev. D* **86**, 075024 (2012), arXiv:1207.0776 [astro-ph.HE].
- [68] S. S. Wilks, The Large-Sample Distribution of the Likelihood Ratio for Testing Composite Hypotheses, *Annals Math. Statist.* **9**, 60 (1938).
- [69] H.-J. Li, J.-G. Guo, X.-J. Bi, S.-J. Lin, and P.-F. Yin, Limits on axion-like particles from Mrk 421 with 4.5-year period observations by ARGO-YBJ and Fermi-LAT, *Phys. Rev. D* **103**, 083003 (2021), arXiv:2008.09464 [astro-ph.HE].
- [70] M. Ajello *et al.* (Fermi-LAT), Search for Spectral Irregularities due to Photon–Axionlike-Particle Oscillations with the Fermi Large Area Telescope, *Phys. Rev. Lett.* **116**, 161101 (2016), arXiv:1603.06978 [astro-ph.HE].
- [71] J. Davies, M. Meyer, and G. Cotter, Constraints on axionlike particles from a combined analysis of three flaring fermi flat-spectrum radio quasars, *Phys. Rev. D* **107**, 083027 (2023).
- [72] R. Essig *et al.*, Working Group Report: New Light Weakly Coupled Particles, in *Snowmass 2013: Snowmass on the Mississippi* (2013) arXiv:1311.0029 [hep-ph].
- [73] V. Anastassopoulos *et al.* (CAST), New CAST Limit on the Axion-Photon Interaction, *Nature Phys.* **13**, 584 (2017), arXiv:1705.02290 [hep-ex].
- [74] C. O’Hare, cajohare/axionlimits: Axionlimits, <https://cajohare.github.io/AxionLimits/> (2020).
- [75] C. A. Manzari, Y. Park, B. R. Safdi, and I. Savoray, Supernova axions convert to gamma-rays in magnetic fields of progenitor stars, arXiv e-prints, arXiv:2405.19393 (2024), arXiv:2405.19393 [hep-ph].
- [76] C. Dessert, D. Dunskey, and B. R. Safdi, Upper limit on the axion-photon coupling from magnetic white dwarf polarization, *Phys. Rev. D* **105**, 103034 (2022), arXiv:2203.04319 [hep-ph].
- [77] D. Noordhuis, A. Prabhu, S. J. Witte, A. Y. Chen, F. Cruz, and C. Weniger, Novel Constraints on Axions Produced in Pulsar Polar-Cap Cascades, *Phys. Rev. Lett.* **131**, 111004 (2023), arXiv:2209.09917 [hep-ph].
- [78] M. Escudero, C. K. Pooni, M. Fairbairn, D. Blas, X. Du, and D. J. E. Marsh, Axion star explosions: A new source for axion indirect detection, *Phys. Rev. D* **109**, 043018 (2024), arXiv:2302.10206 [hep-ph].
- [79] B. Betancourt Kamenetskaia, N. Fraija, and G. Herrera, Polarization measurements as a probe of axion-photon coupling: A study of GRB 221009A, *Phys. Rev. D* **111**, 115008 (2025), arXiv:2408.07352 [hep-ph].
- [80] O. Ning and B. R. Safdi, Leading Axion-Photon Sensitivity with NuSTAR Observations of M82 and M87, *Phys. Rev. Lett.* **134**, 171003 (2025), arXiv:2404.14476 [hep-ph].
- [81] R. Caputo *et al.*, All-sky Medium Energy Gamma-ray Observatory eXplorer mission concept, *J. Astron. Telesc. Instrum. Syst.* **8**, 044003 (2022), arXiv:2208.04990 [astro-ph.IM].
- [82] M. Tavani *et al.* (e-ASTROGAM), Science with e-ASTROGAM: A space mission for MeV–GeV gamma-ray astrophysics, *JHEAp* **19**, 1 (2018), arXiv:1711.01265 [astro-ph.HE].
- [83] B. S. Acharya *et al.* (CTA Consortium), *Science with the Cherenkov Telescope Array* (WSP, 2018) arXiv:1709.07997 [astro-ph.IM].